An interlaced strategy for open circuit voltage and capacity estimation for lithium-ion batteries

1st Domenico Natella
Department of Engineering
University of Sannio
Benevento, Italy
dnatella@unisannio.it

2nd Simona Onori
Department of Energy Resources Engineering
Stanford University
Stanford, CA
sonori@stanford.edu

3rd Francesco Vasca
Department of Engineering
University of Sannio
Benevento, Italy
vasca@unisannio.it

***Abstract*—Performance of battery energy management strategies are largely affected by battery parameters which change depending on real usage during its life. In fact, variations of capacity, open circuit voltage characteristic and internal resistance influence the battery management when cycled. In this paper a technique for the simultaneous real-time co-estimation of the battery parameters is proposed. The estimator consists of a set of interconnected subsystems grounded on the integration of recursive least square techniques and a state of charge observer. The estimator effectiveness is verified by using experiments with charging and discharging cycles of a Li-ion cell during its life.**

I. Introduction

Knowledge of battery degradation due to aging and usage conditions is key for energy management systems in many applications such as electric and hybrid vehicles, smart grids, satellites. Changes in the battery behavior can be captured by means of corresponding variations of its model parameters [1], [2]. It is widely recognized that the state of health (SOH) reduction highlights the loss of the battery charge capacity and is dependent on the usage, e.g., charging/discharging patterns and on the overall cycles or ampere-hour-throughput that the battery has undergone to during its life [3], [4], [5]. Degradation manifests itself not only on the SOH reduction, but also on variations of the open circuit voltage (indicated in the sequel with the variable OCV) vs. state of charge (SOC, indicated in the sequel with the variable z) nonlinear map [6], [7]. The importance of accounting for changes in the dependence of $OCV(z)$ as the battery degrades has been recognized in the literature [8], [9], [10], [11], [12]. Another well known effect of aging and usage conditions is the increase of the internal resistance R_0 [13], [14].

In the literature it has been clearly motivated the importance for an online identification of different parameters during the battery life which led to the use of the term “co-estimation” standing for simultaneous tracking of SOC and variations of the battery parameters. On-board algorithms have been proposed for the simultaneous estimations of SOC and SOH based on reinforcement learning [15] and data-driven approaches [16]. Battery electrochemical models have been used in combination with Kalman filters or sliding mode methods for SOH and SOC estimations, see among others [17], [18], [19]. The real-time feasibility of a sliding-mode electro-based observer grounded in a single particle electrochemical model has also recently been demonstrated in [20].

The co-estimation framework proposed in this paper is based on an equivalent circuit model (ECM) [21], [22] for simultaneous online evaluation of SOC, SOH, identification of the parameters of the polynomial $OCV(z)$ characteristic and tracking of the other equivalent circuit parameters variations during Li-ion battery life. The analysis of this “complete” co-estimation problem is still in its infancy but there exist many studies which consider co-estimation of SOC with specific subsets of the battery parameters [23], so as discussed below.

The co-estimation problem of SOC and ECM parameters has been investigated in [24] where a polynomial approximation of the $OCV(z)$ map with constant coefficients and a fixed capacity are used. A constant capacity is also considered in [25]. The capacity is a fixed parameter also in the co-estimation approach for SOC and ECM parameters proposed in [26] where an offline identified piecewise linear approximation of the $OCV(z)$ map is assumed and in [14] where the coefficients of the $OCV(z)$ characteristic are estimated online. A co-estimation strategy based on a Wiener configuration of the ECM is presented in [27] where the capacity is assumed as a constant and the map $OCV(z)$ is obtained offline by averaging the curves recorded during charging and discharging phases. Many co-estimation studies consider the battery health degradation due to aging. The typical approach used for the online evaluation of SOH is the reduction of the battery capacity. The combined SOC/SOH estimation algorithm presented in [28] requires offline experimental procedures for SOH and internal resistance evaluations. A sliding-mode observer for SOC/SOH estimation has been proposed in [29] but a linear $OCV(z)$ characteristic is assumed. In the Kalman filtering approach proposed in [30] the model parameters are estimated offline by conducting specific driving test at the beginning of service life of the battery. The online estimation of the internal resistance is included in the SOC/SOH algorithm discussed in [31] which requires the knowledge of the slope of the $OCV(z)$ characteristic. A Kalman filter combined with a recursive least-squares (RLS) algorithm for the ECM parameters is proposed in [32] but the equation used for the OCV estimation requires the comparison with a pre-recorded table $OCV(z)$ which is not corrected online. A similar difficulty emerges from the technique proposed in [9] where the errors used for the online adaptations require data for the OCV and the battery capacity. The SOC/SOH and ECM parameters co-estimation problems analyzed in [33], [34], [35] do not consider online adaptations of the OCV map which, instead, is taken into account in our solution. Possible changes of the parameters of the $OCV(z)$ characteristic are not considered in [36] either. The problem of online estimation of the OCV has been investigated in [37], [38] which consider RLS equations where the instantaneous value of the OCV is used as a parameter to be estimated. A similar idea is used in [39]. Differently from our framework, the latter solutions do not consider the fact that the parameters of the $OCV(z)$ curve are expected to change slower than the SOC dynamics.

The literature analysis presented above shows that finding robust solutions to the complete co-estimation problem is still an open issue. This paper provides a contribution in this direction by proposing a new framework where estimators for SOC, SOH, $OCV(z)$ characteristic and ECM parameters can be separately designed and simultaneously (or independently) activated while keeping the calibration effort low. The rest of the paper is organized as follows. In Section II the ECM of a battery cell is recalled. In Section III the proposed estimator is discussed. Section IV presents the estimation results whose effectiveness is verified by using battery experimental data. Finally, in Section V the conclusions of our study are summarized.

II. Equivalent circuit dynamic model

The equivalent electrical circuit of the battery (cell) considered in our analysis is shown in Fig. 1, where i_b is the battery current assumed to be positive during discharge, e_b is the voltage at the battery terminals, e_ℓ is the voltage across the capacitor which captures the battery dynamics in the $R_\ell C_\ell$ branches, $\ell = 1, \dots, L$, OCV is the open circuit voltage, R_0 is the internal resistance. By applying the Kirchhoff's laws to the circuit in Fig. 1 the following continuous-time model is obtained

$$\dot{e}_\ell = -\frac{1}{R_\ell C_\ell} e_\ell + \frac{1}{C_\ell} i_b, \quad \ell = 1, \dots, L \tag{1a}$$

$$\dot{z} = -\frac{1}{Q} i_b \tag{1b}$$

$$e_b = OCV(z) - \sum_{\ell=1}^{L} v_\ell - R_0 i_b \tag{1c}$$

where the voltages e_ℓ, $\ell = 1, \dots, L$, and the state of charge z are the state variables whose continuous-time derivatives have been indicated with $\dot{e}_\ell$ and $\dot{z}$, respectively, i_b is the model input and e_b is the output. The parameter Q is the battery capacity which determines the state of health as the ratio Q/Q^* where Q^* is the nominal capacity of a fresh battery. The function $OCV(z)$ represents the nonlinear dependence of the open circuit voltage on the SOC.

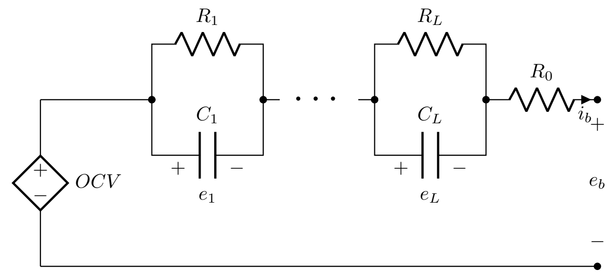

Fig. 1. Equivalent circuit model of the battery cell.

By discretizing (1) with the forward-Euler method one obtains

$$e_\ell(k+1) = \left(1 - \frac{h}{R_\ell C_\ell}\right) e_\ell(k) + \frac{h}{C_\ell} i_b(k) \tag{2a}$$

$$z(k+1) = z(k) - \frac{h}{Q} i_b(k) \tag{2b}$$

$$e_b(k) = OCV(z(k)) - \sum_{\ell=1}^{L} e_\ell(k) - R_0 i_b(k) \tag{2c}$$

for $\ell = 1, \dots, L$, where $k \in \mathbb{N}$ is the discrete-time step, $h \in \mathbb{R}_+$ is the sampling period and the initial conditions $e_\ell(0)$ and $z(0)$ are given. The map of OCV vs. SOC is approximated by a polynomial function. Specifically, one can write:

$$OCV(z) = \sum_{p=0}^{P} a_p z^p \tag{3}$$

where $a_p \in \mathbb{R}$, $p = 0 \dots, P$ and $P \in \mathbb{N}$ is the desired order of the polynomial.

Note that by assuming $P = 1$ in (3) and by substituting the resulting expressions in (2c), the model (2) can be written in the following linear discrete-time state space form

$$\xi(k+1) = A\xi(k) + B i_b(k) \tag{4a}$$

$$e_b(k) = c^\top \xi(k) - R_0 i_b(k) + a_0 \tag{4b}$$

for $k \in \mathbb{N}$, where $\xi = (e_1 \, \dots \, e_L \; z)^\top$ is the state vector, $c^\top$ indicates the transpose of the vector c, and the matrices of the model are given by

$$A = diag\left(\begin{array}{cccc} 1 - \frac{h}{R_1 C_1} & \dots & 1 + \frac{h}{R_L C_L} & 1 \end{array} \right) \tag{5a}$$

$$B = \left(\begin{array}{cccc} \frac{h}{C_1} & \dots & \frac{h}{C_L} & -\frac{h}{Q} \end{array} \right)^\top \tag{5b}$$

$$c^\top = -\left(\begin{array}{cccc} 1 & \dots & 1 & -a_1 \end{array} \right) \tag{5c}$$

where $diag(v)$ stands for a diagonal matrix whose elements on the diagonal are given by the elements of the vector v. The model (2) is the basis for the design of the gains of the SOC observer presented in next section as part of the proposed estimator.

III. Proposed estimator

The proposed estimation technique consists of the integration of the SOC, SOH, R_0 and OCV estimators. The estimator exploits in different forms the RLS equations which can be written in the following general form

$$\Sigma(k) = \mu\Sigma(k-1) + \gamma(k)\gamma(k)^\top \tag{6a}$$

$$\hat{\pi}(k) = \hat{\pi}(k-1) + \Sigma(k)^{-1}\gamma(k)\left(y(k) - \gamma(k)^\top\hat{\pi}(k-1)\right) \tag{6b}$$

where $y(k) = \gamma(k)^\top\pi + \epsilon(k)$, $\epsilon(k)$ is the error, $y(k)$ and the regression vector $\gamma(k)$ are known quantities, π is the vector of the parameters and μ is the forgetting factor.

Note that, in the following the generic vector $\hat{\pi}(k)$ corresponds to different model parameters whether the RLS expressions (6) are applied for the estimations of the parameters of the $OCV(z)$ characteristic, the resistance R_0 and the battery capacity Q.

The estimated parameters $\hat{a}_p$, $p = 0, 1, \ldots, P$, in (3) and $\hat{R}_0$ are approximated with their moving average which can be written as $\hat{\alpha}_p = \frac{1}{N}\sum_{s=k-N+1}^{k}\hat{a}_p(s)$ and $\hat{\beta}_0 = \frac{1}{N}\sum_{s=k-N+1}^{k}\hat{R}_0(s)$, respectively. The estimation of $\hat{\alpha}_p$, $p = 0, 1, \ldots, P$, and $\hat{\beta}_0$ is performed by taking the moving average on both sides of (2c) after substituting (3). By assuming slowly varying variations of the parameters, the moving average of the products $\hat{a}_p\hat{z}^p$, $p = 0, 1, \ldots, P$, and $\hat{R}_0 i_b$ can be approximated with the products of the corresponding moving averages [40] and one can implement the RLS equations (6) by choosing

$$\hat{\pi}(k)^\top = \begin{pmatrix} \hat{\alpha}_0(k) & \ldots & \hat{\alpha}_P(k) & \hat{\beta}_0(k) \end{pmatrix}, \tag{7}$$

together with

$$y(k) = \frac{1}{N}\sum_{s=k-N+1}^{k}\left[e_b(s) + \sum_{\ell=1}^{L}\hat{e}_\ell(s)\right] \tag{8a}$$

$$\gamma(k) = \frac{1}{N}\sum_{s=k-N+1}^{k}\begin{pmatrix} 1 \\ \hat{z}(s) \\ \vdots \\ (\hat{z}(s))^P \\ i_b(s) \end{pmatrix} \tag{8b}$$

for $k \geq N$. The expressions (7)–(8) are obtained by applying moving averages with a horizon of N steps to the model (2)–(3) and by substituting the variables e_ℓ, $\ell = 1, \ldots, L$ and z with the corresponding estimations $\hat{e}_\ell$, $\ell = 1, \ldots, L$ and $\hat{z}$ from the SOC observer.

The battery capacity estimation $\hat{Q}$ is obtained by applying to (2b) the moving average with a horizon of N steps and then by implementing (6) with $\hat{\pi}(k) = \hat{Q}(k)$ and

$$y(k) = -\sum_{s=k-N}^{k-1} i_b(s) \tag{9a}$$

$$\gamma(k) = \hat{z}(k) - \hat{z}(k-N) \tag{9b}$$

for $k \geq N$.

The SOC observer is interconnected with the RLS algorithms used for the estimation of the battery capacity and the parameters of the $OCV(z)$ characteristic and R_0. In particular, from (2)–(3) the SOC observer equations are:

$$\hat{e}_\ell(k+1) = \left(1 - \frac{h}{R_\ell C_\ell}\right)\hat{e}_\ell(k) + \frac{h}{C_\ell}i_b(k) + g_\ell(e_b(k) - \hat{e}_b(k)) \tag{10a}$$

$$\hat{z}(k+1) = \hat{z}(k) - \frac{h}{\hat{Q}(k)}i_b(k) + g_{L+1}(e_b(k) - \hat{e}_b(k)) \tag{10b}$$

$$\hat{e}_b(k) = \sum_{p=0}^{P}\hat{\alpha}_p(k)\hat{z}(k)^p - \sum_{\ell=1}^{L}\hat{e}_\ell(k) - \hat{\beta}_0(k)i_b(k) \tag{10c}$$

for $\ell = 1, \ldots, L$, $k \in \mathbb{N}$, where the parameters $\hat{Q}(k)$, $\hat{\alpha}_p(k)$, $p = 0, 1, \ldots, P$, and $\hat{\beta}_j$, $j = 0, 1, \ldots, J$, are obtained from the RLS algorithms described above.

In the particular case $P = 1$ the model (2) is linear and the observer gains g_ℓ, $\ell = 1, \ldots, L+1$ can be designed with classical techniques for linear systems. To this aim the observability of the system can be verified by considering the observability matrix of the model (4) which is given by

$$\mathcal{O} = \begin{pmatrix} c^\top \\ c^\top A \\ \vdots \\ c^\top A^L \end{pmatrix} = -\begin{pmatrix} 1 & \ldots & 1 & -a_1 \\ 1 - \frac{h}{R_1 C_1} & \ldots & 1 - \frac{h}{R_L C_L} & -a_1 \\ \vdots & \vdots & \vdots & \vdots \\ \left(1 - \frac{h}{R_1 C_1}\right)^L & \ldots & \left(1 - \frac{h}{R_L C_L}\right)^L & -a_1 \end{pmatrix} \tag{11}$$

where the matrices A and $c^\top$ are given by (5). It is easy to verify that for almost all nonzero a_1 and h, if $R_i C_i \neq R_j C_j$ for any $i \neq j$, the matrix (11) is full rank. Therefore, a possible design rule for the observer vector gain $g \in \mathbb{R}^{L+1}$ consists of assigning the desired eigenvalues to the dynamic matrix of the observer (2), i.e. $A - gc^\top$ where $g = (g_1 \ \ldots \ g_{L+1})^\top$.

IV. Estimation results

The effectiveness of the proposed estimator is verified over experimental data collected for a cylindrical LG M50T INR21700 Li-ion cell with NMC cathode chemistry, nominal voltage 3.63 V, nominal capacity $Q^* = 4.85$ A h. Experiments were carried out at the Stanford Energy Control Laboratory in the Energy Resources Engineering Department at Stanford University [41]. The aging campaign consists in subjecting the battery to a real driving profile. Periodic characterization tests, i.e. Capacity test and Hybrid Pulse Power Characterization (HPPC) test, were performed to assess battery health. Every 50 aging cycles a capacity test and a HPPC test are performed. The former consists of a $C/20$ constant discharge and the latter consists of charge and discharge pulses at different SOC. Algorithm 1 synthesizes the procedure for the aging campaign where the integer n is the number of the aging tests already performed and the entire campaign is stopped when n reaches the parameter $n_{\max}$. The occurrence of the characterization tests is expressed by the condition $n = 25 + 50\nu$ where ν is the number of Capacity/HPPC tests already performed.

Algorithm 1: Aging campaign

Parameter: $n_{\max}$
Input : z
Initialize : $n = 0, \nu = 0$
begin
  $CC - CV$ standard charging protocol;
  while $n \leq n_{\max}$ **do**
    while $z \geq 0.8$ **do**
      $CC(at\ C/4)$ discharge;
    end
    while $z \geq 0.2$ **do**
      UDDS driving cycle;
    end
    if $n = 25 + 50\nu$ **then**
      Capacity test (C/20) AND HPPC test;
      $\nu = \nu + 1$;
    end
    $n = n + 1$;
    while $z \leq 0.8$ **do**
      $CC(at\ 3C) - CV(at\ 4V)$ charge;
    end
    while $z \leq 1$ **do**
      $CC(at\ C/4) - CV(at\ 4.2V)$ charge;
    end
  end
end

A. Model parameters determination

The benchmark values of the battery capacity have been obtained by using the measurements of the capacity tests. In particular, for a discharging current i_b and a time interval Δt for the discharge the capacity can be evaluated as $Q = i_b \Delta t$. The values obtained for the battery under test are detailed in next subsection. The HPPC test is used for the determination of the benchmark values for the model parameters. The benchmark values for the resistance R_0 for the fresh battery and after cycling are obtained by computing the voltage discontinuities, say Δ_v, in correspondence to the step changes of the current, say Δ_i. By applying least square estimations to the set of voltage-current discontinuity pairs obtained in the HPPC tests the following benchmark values have been obtained: $0.0265\,\Omega$ for the fresh battery and $0.0286\,\Omega$ after 200 cycles. The values of R_1 and C_1 are obtained by considering the time intervals of the transients during the relaxation phases of the HPPC tests and the corresponding steady state voltages [21]. The experimental data allow us to calibrate $R_1 = 0.016\,\Omega$ and $C_1 = 0.036\,\mathrm{F}$.

Two sections of the aging test at different aging stages have been used to verify the estimation performance of the proposed integrated estimator. The estimator parameters are: $g_1 = 0.5$, $g_2 = 0.001$, $\mu = 0.99$ for both RLS estimators. For the estimator of α_p with $p = 0, ..., P$ and β_0 it is $\Sigma(0)$ equal to the identity matrix of dimension $(P+1) \times (P+1)$. For the estimator of Q it is $\Sigma(0) = 1$. All initial conditions for estimated states and parameters are assigned equal to zero unless otherwise noted.

B. Discharge validation test

The proposed estimation strategy has been validated over the current and voltage profiles shown in Fig. 2, which are part of the aging tests performed during the aging campaign, at different aging stages of the battery.

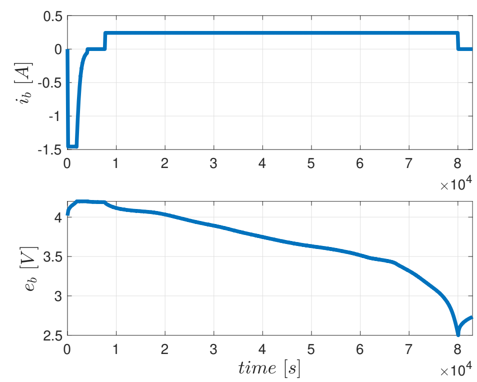

Fig. 2. Battery current i_b (top) and voltage e_b (bottom) profiles for the first validation test of the estimator applied to the fresh battery.

The estimated state of charge is shown in Fig. 3. The RMS of the estimation error $z - \hat{z}$ for the fresh battery is $6.8 \cdot 10^{-3}$ while for the aged one is $2.1 \cdot 10^{-3}$.

For the polynomial approximation of the $OCV(z)$ map a fifth order polynomial, i.e., $P = 5$, has been chosen. The estimation of α_p, $p = 0, ..., P$ are shown in Fig. 2. The parameters estimation captures the variation of the $OCV(z)$ characteristic due to the battery aging, so as shown in Fig. 5 where the characteristics are reported for the fresh battery and after 200 cycles. The reference $OCV(z)$ maps are obtained through a discharge operation at $C/20$ when the battery is considered as new one and after 200 cycles. The RMS error of the polynomial approximations are $1.1 \cdot 10^{-3}$ and $1.7 \cdot 10^{-3}$, respectively.

The time evolution of the battery capacity estimations for the tests carried out when the battery is fresh and after 200 cycles are shown in Fig. 6. The benchmark values of the battery capacity have been obtained by using the measurements of the capacity tests. In particular, for the fresh battery it is $i_b = 24.33\,\mathrm{mA}$ and the duration of the test is $19.95\,\mathrm{h}$ which corresponds to a capacity equal to $Q_0 = 4.8538\,\mathrm{A\,h}$. The estimated value of the capacity at steady state is $\hat{Q}_0 = 4.8742\,\mathrm{A\,h}$ which corresponds to a relative percentage error of 0.4%. For the capacity test after 200 cycles the same battery current is used and the duration of the test is $19.14\,\mathrm{h}$ which corresponds to a capacity equal to $Q_{200} = 4.6568\,\mathrm{A\,h}$. The estimated value

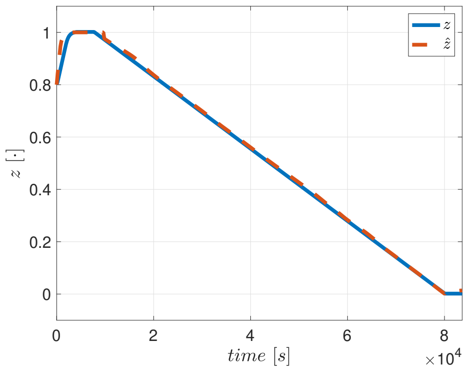

Fig. 3. Real (blue, continuous) and estimated (red, dashed) state of charge for the discharge validation test when the battery is fresh.

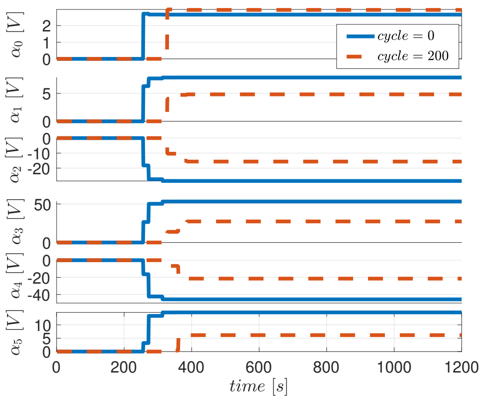

Fig. 4. The estimations of the parameters α_p $p = 0, ..., 5$ activated during the test in Fig. 2 which has been implemented at the beginning of battery life (blue, continuous) and after 200 cycles (red, dashed).

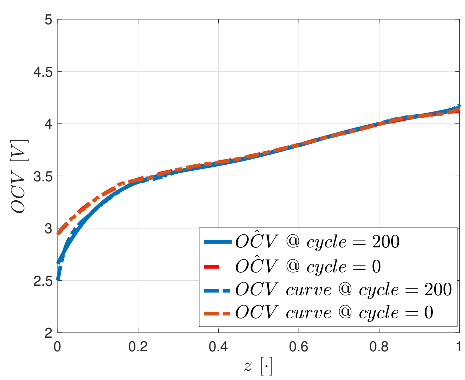

Fig. 5. $O\hat{C}V(z)$ evaluated at the beginning of battery life (blue, continuous) and after 200 cycles (red, dashed). The corresponding benchmark values are represented with dashed-dotted lines, blue and red, respectively.

of the capacity at steady state is $\hat{Q}_{200} = 4.6425\,\mathrm{A\,h}$ which corresponds to a relative percentage error equal to 0.3%.

The series resistance estimations are shown in Fig. 7. The steady state values of the estimated resistance obtained with the proposed procedure are $0.0268\,\Omega$ for the fresh battery and $0.0295\,\Omega$ after 200 cycles. The relative percentage errors of the estimated values with respect to the corresponding benchmarks obtained from the HPPC tests are 1.1% and 3.1%, respectively.

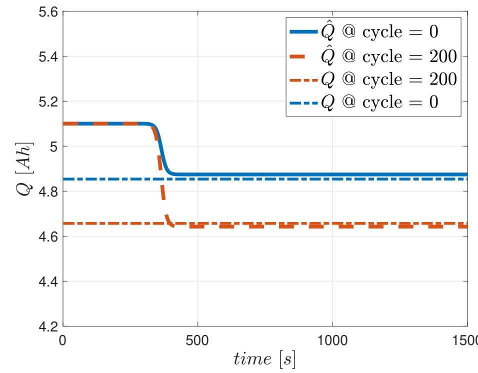

Fig. 6. Battery capacity $\hat{Q}$ evaluated during the discharge validation test at the beginning of battery life (blue, continuous) and after 200 cycles (red, dashed). The corresponding benchmark values are represented with dashed-dotted lines, blue and red, respectively.

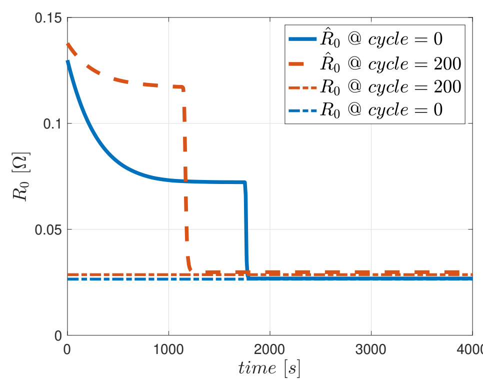

Fig. 7. Series resistance $\hat{R}_0$ evaluated during the discharge validation test at the beginning of battery life (blue, continuous) and after 200 cycles (red, dashed). The corresponding benchmark values are represented with dashed-dotted lines, blue and red, respectively.

V. Conclusion

A co-estimation technique for battery parameters (capacity, open circuit voltage vs. state of charge characteristic, internal resistance) combined with a state of charge observer has been proposed. The estimator exploits the application of moving average functions to the equivalent circuit model of a battery cell. Experimental results show the effectiveness of the proposed solution during battery discharging tests over battery life. Future research will focus on validating the proposed strategy in complete driving cycles and more complex testing scenarios, in the direction traced by the authors in [42].

References

[1] G. L. Plett, "Recursive approximate weighted total least squares estimation of battery cell total capacity," J. Power Sources, vol. 196, no. 4, pp. 2319–2331, 2011.

[2] S. Baccari, F. Vasca, E. Mostacciuolo, L. Iannelli, S. Sagnelli, R. Luisi, and V. Stanzione, "A characterization system for LEO satellites batteries," in Proceedings of the IEEE European Space Power Conference, Juan-les-Pins, France, 30 Sep.-4 Oct. 2019, pp. 1–6.

[3] M. Berecibar, I. Gandiaga, I. Villarreal, N. Omar, J. Van Mierlo, and P. Van den Bossche, "Critical review of state of health estimation methods of Li-ion batteries for real applications," Ren. and Sust. Energy Reviews, vol. 56, pp. 572–587, 2016.

[4] Energy Vehicle Technologies Program, U.S. Department of Energy, "United States Advanced Battery Consortium Battery Test Manual For Electric Vehicles," INL/EXT-15-34184, 2020.

[5] J. Tian, R. Xiong, and Q. Yu, "Fractional-Order Model-Based Incremental Capacity Analysis for Degradation State Recognition of Lithium-Ion Batteries," IEEE Trans. Ind. Electron., vol. 66, no. 2, pp. 1576–1584, 2019.

[6] A. Farmann and D. U. Sauer, "A study on the dependency of the open-circuit voltage on temperature and actual aging state of lithium-ion batteries," J. Power Sources, vol. 347, pp. 1–13, 2017.

[7] T. Ouyang, P. Xu, J. Lu, X. Hu, B. Liu, and N. Chen, "Coestimation of State-of-Charge and State-of-Health for Power Batteries Based on Multithread Dynamic Optimization Method," IEEE Trans. Ind. Electron., vol. 69, no. 2, pp. 1157–1166, 2022.

[8] H. Rahimi-Eichi, F. Baronti, and M.-Y. Chow, "Online Adaptive Parameter Identification and State-of-Charge Coestimation for Lithium-Polymer Battery Cells," IEEE Trans. Ind. Electron., vol. 61, no. 4, pp. 2053–2061, 2013.

[9] C. Zhang, X. Li, W. Chen, G. G. Yin, and J. Jiang, "Robust and adaptive estimation of state of charge for Lithium-ion batteries," IEEE Trans. Ind. Electron., vol. 62, no. 8, pp. 4948–4957, 2015.

[10] A. Klintberg, C. Zou, B. Fridholm, and T. Wik, "Kalman filter for adaptive learning of two-dimensional look-up tables applied to OCV-curves for aged battery cells," Control Eng. Practice, vol. 84, pp. 230–237, 2019.

[11] L. Lavigne, J. Sabatier, J. M. Francisco, F. Guillemard, and A. Noury, "Lithium-ion Open Circuit Voltage (OCV) curve modelling and its ageing adjustment," J. Power Sources, vol. 324, pp. 694–703, 2016.

[12] K. Li, F. Wei, K.-J. Tseng, and B.-H. Soong, "A practical lithium-ion battery model for state of energy and voltage responses prediction incorporating temperature and ageing effects," IEEE Trans. Ind. Electron., vol. 65, no. 8, pp. 6696–6708, 2018.

[13] D.-I. Stroe, M. Swierczynski, S. K. Kær, and R. Teodorescu, "Degradation behavior of lithium-ion batteries during calendar ageing – The case of the internal resistance increase," IEEE Trans. Ind. Applications, vol. 54, no. 1, pp. 517–525, 2017.

[14] H. Rahimi-Eichi, F. Baronti, and M.-Y. Chow, "Online Adaptive Parameter Identification and State-of-Charge Coestimation for Lithium-Polymer Battery Cells," IEEE Trans. Ind. Electron., vol. 61, no. 4, pp. 2053–2061, 2014.

[15] D. Natella and F. Vasca, "Battery State of Health Estimation via Reinforcement Learning," in Proceedings of the European Control Conference, Delft, Netherlands, 29 June-2 July 2021, pp. 1651–1656.

[16] Y. Song, D. Liu, H. Liao, and Y. Peng, "A hybrid statistical data-driven method for on-line joint state estimation of lithium-ion batteries," Applied Energy, vol. 261, p. 114408, 2020.

[17] O. Barbarisi, F. Vasca, and L. Glielmo, "State of charge Kalman filter estimator for automotive batteries," Control Eng. Practice, vol. 14, no. 3, pp. 267–275, 2006.

[18] D. Di Domenico, A. Stefanopoulou, and G. Fiengo, "Lithium-Ion Battery State of Charge and Critical Surface Charge Estimation Using an Electrochemical Model-Based Extended Kalman Filter," J. Dynamic Systems, Measurement, and Control, vol. 132, no. 6, pp. 061 302–1 – 061 302–11, 2010.

[19] A. Allam and S. Onori, "Online Capacity Estimation for Lithium-Ion Battery Cells via an Electrochemical Model-Based Adaptive Interconnected Observer," IEEE Trans. Control Systems Technology, vol. 29, no. 4, pp. 1636–1651, 2021.

[20] A. Allam, E. Catenaro, and S. Onori, "Pushing the Envelope in Battery Estimation Algorithms," Iscience, vol. 23, no. 12, p. 101847, 2020.

[21] G. L. Plett, Battery management systems, Volume II: Equivalent-circuit methods. Artech House, 2015.

[22] S. Baccari, S. Sagnelli, L. Iannelli, and F. Vasca, "A Switched Electrical Model with Thermal Effects for Li-ion Batteries," in Proceedings of the European Control Conference, Delft, Netherlands, 29 June-2 July 2021, pp. 1271–1276.

[23] Y. Wang, J. Tian, Z. Sun, L. Wang, R. Xu, M. Li, and Z. Chen, "A comprehensive review of battery modeling and state estimation approaches for advanced battery management systems," Ren. and Sust. Energy Reviews, vol. 131, p. 110015, 2020.

[24] Z. Wei, G. Dong, X. Zhang, J. Pou, Z. Quan, and H. He, "Noise-Immune Model Identification and State-of-Charge Estimation for Lithium-Ion Battery Using Bilinear Parameterization," IEEE Trans. Ind. Electron., vol. 68, no. 1, pp. 312–323, 2021.

[25] J. Meng, D.-I. Stroe, M. Ricco, G. Luo, and R. Teodorescu, "A Simplified Model-Based State-of-Charge Estimation Approach for Lithium-Ion Battery With Dynamic Linear Model," IEEE Trans. Ind. Electron., vol. 66, no. 10, pp. 7717–7727, 2019.

[26] Z. Wei, C. Zou, F. Leng, B. H. Soong, and K.-J. Tseng, "Online Model Identification and State-of-Charge Estimate for Lithium-Ion Battery With a Recursive Total Least Squares-Based Observer," IEEE Trans. Ind. Electron., vol. 65, no. 2, pp. 1336–1346, 2018.

[27] F. Naseri, E. Schaltz, D.-I. Stroe, A. Gismero, and E. Farjah, "An Enhanced Equivalent Circuit Model With Real-Time Parameter Identification for Battery State-of-Charge Estimation," IEEE Trans. Ind. Electron., vol. 69, no. 4, pp. 3743–3751, 2021.

[28] Y. Zou, X. Hu, H. Ma, and S. E. Li, "Combined State of Charge and State of Health estimation over lithium-ion battery cell cycle lifespan for electric vehicles," J. Power Sources, vol. 273, pp. 793–803, 2015.

[29] M. Gholizadeh and F. R. Salmasi, "Estimation of State of Charge, Unknown Nonlinearities, and State of Health of a Lithium-Ion Battery Based on a Comprehensive Unobservable Model," IEEE Trans. Ind. Electron., vol. 61, no. 3, pp. 1335–1344, 2013.

[30] W. Yan, B. Zhang, G. Zhao, S. Tang, G. Niu, and X. Wang, "A Battery Management System With a Lebesgue-Sampling-Based Extended Kalman Filter," IEEE Trans. Ind. Electron., vol. 66, no. 4, pp. 3227–3236, 2018.

[31] Y. Feng, C. Xue, Q.-L. Han, F. Han, and J. Du, "Robust Estimation for State-of-Charge and State-of-Health of Lithium-Ion Batteries Using Integral-Type Terminal Sliding-Mode Observers," IEEE Trans. Ind. Electron., vol. 67, no. 5, pp. 4013–4023, 2019.

[32] S. Li, K. Li, E. Xiao, and C.-K. Wong, "Joint SoC and SoH Estimation for Zinc–Nickel Single-Flow Batteries," IEEE Trans. Ind. Electron., vol. 67, no. 10, pp. 8484–8494, 2020.

[33] X. Hu, H. Yuan, C. Zou, Z. Li, and L. Zhang, "Co-Estimation of State of Charge and State of Health for Lithium-Ion Batteries Based on Fractional-Order Calculus," IEEE Trans. Vehicular Technology, vol. 67, no. 11, pp. 10 319–10 329, 2018.

[34] R. Xiong, J. Wanga, W. Shen, J. Tian, and H. Mua, "Co-Estimation of State of Charge and Capacity for Lithium-Ion Batteries with Multi-Stage Model Fusion Method," Engineering, vol. 7, pp. 1469–1482, 2021.

[35] D. Xiao, G. Fang, S. Liu, S. Yuan, R. Ahmed, S. Habibi, and A. Emadi, "Reduced-Coupling Coestimation of SOC and SOH for Lithium-Ion Batteries Based on Convex Optimization," IEEE Trans. Power Electron., vol. 35, no. 11, pp. 12 332–12 346, 2020.

[36] X. Hu, H. Jiang, F. Feng, and B. Liu, "An enhanced multi-state estimation hierarchy for advanced lithium-ion battery management," Applied Energy, vol. 257, p. 114019, 2020.

[37] P. Shen, M. Ouyang, L. Lu, J. Li, and X. Feng, "The Co-estimation of State of Charge, State of Health, and State of Function for Lithium-Ion Batteries in Electric Vehicles," IEEE Trans. Vehicular Technology, vol. 67, no. 1, pp. 92–103, 2018.

[38] S. Zhang and X. Zhang, "A multi time-scale framework for state-of-charge and capacity estimation of lithium-ion battery under optimal operating temperature range," J. Energy Storage, vol. 35, p. 102325, 2021.

[39] S. Zhang, X. Guo, and X. Zhang, "A novel one-way transmitted co-estimation framework for capacity and state-of-charge of lithium-ion battery based on double adaptive extended Kalman filters," J. Energy Storage, vol. 33, p. 102093, 2021.

[40] L. Iannelli, K. H. Johansson, U. T. Jönsson, and F. Vasca, "Averaging of nonsmooth systems using dither," Automatica, vol. 42, no. 4, pp. 669–676, 2006.

[41] G. Pozzato, A. Allam, and S. Onori, "Lithium-ion battery aging dataset based on electric vehicle real-driving profiles," Data in Brief, vol. 41, p. 107995, 2022.

[42] D. Natella, S. Onori, and F. Vasca, "A co-estimation framework for state of charge and parameters of lithium-ion battery with robustness to aging and usage conditions," IEEE Trans. Ind. Electron., 2022, Accepted for publication, early access DOI: 10.1109/TIE.2022.3194576.